Journal of Radioanalytical and Nuclear Chemistry (2019) 322:817–825
https://doi.org/10.1007/s10967-019-06722-3

Measurement and covariance analysis of ^{232}Th(n, 2n)^{231}Th reaction cross section

Meghna Karkera[1] · Santhi Sheela Yerraguntla[2] · Sripathi Punchithaya[3,4] · Saraswatula Venkata Suryanarayana[5] · Manjunatha Prasad Karantha[1,6] · Haladhara Naik[7] · Srinivasan Ganesan[8] · Laxman Singh Dhanu[5] · Rajeev Kumar[9] · Kapil Deo[10] · Devesh Raj[9] · Tarun Patel[11] · Saroj Bishnoi[11] · Umasankari Kannan[9]

Received: 19 June 2019 / Published online: 24 August 2019

Abstract

The ^{232}Th(n, 2n)^{231}Th reaction cross sections were measured at the neutron energies of 10.49 ± 0.29, 14.46 ± 0.26, 18.36 ± 0.24 MeV and 15.03 ± 0.003 MeV. For the first three energies, ^{7}Li(p, n) reaction as a neutron source at the BARC-TIFR Pelletron accelerator facility was used. For the latter energy, ^{3}H(d, n) neutron source using the PURNIMA neutron generator facility was used. The experiments were carried out using the activation method and off-line γ-ray spectrometric technique. Covariance information of various attributes of cross section was propagated to obtain the covariance matrix for the reaction cross sections. The experimental resuts obtained with reference to the two different neutron sources are then compared with the values of evaluated nuclear data files such as ENDF/B-VIII.0, JENDL 4.0, JEFF-3.2, ROSFOND-2010, TENDL-2017 and the theoretical values from TALYS-1.9 code.

Keywords ^{232}Th(n, 2n)^{231}Th reaction cross section · Activation and off-line γ-ray spectrometric technique · Covariance analysis

✉ Haladhara Naik
naikhbarc@yahoo.com

1 Department of Data Science, Manipal Academy of Higher Education, Manipal 576104, India

2 Department of MACS, National Institute of Technology Karnataka, Surathkal 575025, India

3 Department of Physics, MIT, Manipal 576104, India

4 NIE, Mysuru 570008, India

5 Nuclear Physics Division, Bhabha Atomic Research Centre, Mumbai 400085, India

6 CARAMS, Manipal Academy of Higher Education, Manipal 576104, India

7 Formerly in Radiochemistry Division, Bhabha Atomic Research Centre, Mumbai 400085, India

8 Former Raja Ramanna Fellow of the DAE, Bhabha Atomic Research Centre, Mumbai 400085, India

9 Reactor Physics Design Division, Bhabha Atomic Research Center, Mumbai 400085, India

10 Safety Studies Section, Bhabha Atomic Research Centre, Mumbai 400085, India

11 Technical Physics Division, Bhabha Atomic Research Centre, Mumbai 400085, India

Introduction

Neutron induced reaction and fission cross sections of isotopes of actinides from Th–Cm are important for various types of reactor applications. In particular the (n, γ) and (n, 2n) reaction cross-sections of uranium and plutonium isotopes are important for the conventional light and heavy water reactors as well as for the fast reactor [1, 2]. On the other hand, the (n, γ) and (n, 2n) reaction cross-sections of thorium isotopes are important for advanced heavy water reactor (AHWR) [3] and the accelerator driven sub-critical system (ADSs) [4–6]. In AHWR, one of the hazardous actinide is ^{232}U, which has daughter products with high energy gamma-lines and thus creates a problem of safety issue. The actinide, ^{232}U is being produced from different reaction routes. One of the main reactions leading to the production of ^{232}U in thorium loaded reactors is ^{232}Th(n, 2n)^{231}Th reaction. The actinide, ^{231}Th decays by beta particle emission and produces ^{231}Pa. The (n, γ) reaction of ^{231}Pa produces ^{232}Pa, which decays by beta particle emission and gives rise to ^{232}U. So an assessment of the amount of ^{232}U produced in thorium fuel cycle requires an accurate knowledge of ^{232}Th(n, 2n)^{231}Th reaction cross section data at different neutron energies. The existing experimental and evaluated data for the ^{232}Th(n, 2n)^{231}Th reaction cross section shows large discrepancies within the neutron energies from 8 to 15 MeV. Thus, there is a need for more precise and accurate measurements of cross sections with covariance analysis.

In the present work, we obtain the ^{232}Th(n, 2n)^{231}Th reaction cross section with covariance error matrix at the effective neutron energies of 10.49 ± 0.29, 14.46 ± 0.26 and 18.36 ± 0.24 MeV, employing the ^{7}Li(p, n) reaction as the neutron source using the BARC-TIFR Pelletron accelerator facility. Since ^{7}Li(p, n) based neutron source has a broad neutron spectrum, we have considered a quasi mono-energetic source by employing ^{3}H(d, n) reaction using the PURNIMA Neutron Generator facility for the same reaction. The energy of neutron beam generated by this facility is 15.03 ± 0.003 MeV. We observe whether measurements obtained using different types of neutron sources behaves similar while comparing with the recommended curves. For the experiment involving the ^{7}Li(p, n) reaction as the neutron source, ^{97}Zr fission product characterised by the γ-line with 743.3 keV energy, was used as the monitor nuclide. For the experiment involving the ^{3}H(d, n) reaction as neutron source, ^{115m}In characterised by the γ-line with 336.2 keV energy was used as the monitor nuclide. In both the experiments, ^{231}Th reaction product characterised by the γ-line with 84.21 keV energy was identified as sample nuclide. Table 1 presents the decay data of radionuclides required for estimating ^{232}Th(n, 2n)^{231}Th reaction cross section.

Experimental details

Experiment involving the ^{7}Li(p, n) neutron source

The experiments employing the ^{7}Li(p, n) reaction as a neutron source were performed at the 14 UD BARC-TIFR Pelletron facility [7]. The thickness of natural lithium foil used in the experiment to produce neutrons is 3.7 mg/cm^2. The natural lithium foil is covered by tantalum foils in the front and the back. The thicknesses of the front tantalum foil and back tantalum foil are 3.9 mg/cm^2 and 41 mg/cm^2, respectively. Behind the Ta–Li–Ta stack, three thorium metal foils of sizes 0.4, 0.5 and 0.5 cm^2 were used for neutron irradiations. The weights of Th metal foils are 211.3, 216.6 and 246.8 mg. The Th–metal foils were wrapped with 0.025 mm thick super pure Al foil. The aluminum wrapped thorium samples were then mounted one at a time at an angle of 0° with respect to the proton beam's direction at a distance of 2.1 cm behind the Ta–Li–Ta stack. The experimental set up used in the present work is given in Fig. 1. Three different irradiations were carried out with the neutrons beam produced from the ^{7}Li(p, n) reaction by using the proton beams of 13, 17 and 21 MeV energies from the accelerator. The protons currents during the irradiations were 55, 90 and 150 nA corresponding to the proton energies of 13, 17 and 21 MeV, respectively. The above mentioned samples were irradiated for the durations of 33,000, 38,400 and 18,000 s. The irradiated samples were then cooled for 237,520, 129,743, 110,580 s. Then the γ-ray counting of the irradiated Al wrapped Th sample was performed by using a pre-calibrated 80-cc HPGe detector coupled to a PC-based 4096 channel analyzer. The resolution of the detector system had a full width at half maximum (FWHM) of 1.8 keV at the 1332.5 keV peak of ^{60}Co. The counting dead time was always kept lesser than 5% by placing the irradiated thorium samples at a distance of 1 cm from the end cap of the detector. The energy and efficiency calibration of the detector system were performed by using standard ^{133}Ba and ^{152}Eu sources, keeping the same geometry.

Experiment involving the ^{3}H(d, n) neutron source

A Schematic diagram of the experimental set up for the neutron irradiation set up based on the ^{3}H(d, n) reaction is given in Fig. 2. This experiment was performed with the neutrons produced by bombarding a tritium target of about 6–8 Curie with deuterons beam of 0.16 MeV. The Cockcroft and Walton type multiplier accelerator available at the PURNIMA Neutron Generator (PNG) facility [8] was employed. The

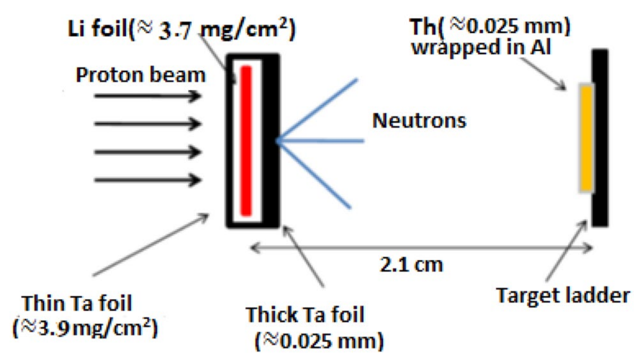

Fig. 1 Schematic representation of the experimental set up for the neutron induced reaction performed at the BARC-TIFR Pelletron facility

Table 1 Decay data of radionuclides required for estimating $\sigma_U(E_n)$

Element	Isotopic abundance	Isotope	Half-life (h)	γ-Ray energy (keV)	γ-Ray abundance
Th	1	^{97}Zr	16.749 ± 0.008	743.3 ± 0.03	0.9309 ± 0.0016
		^{231}Th	24.52 ± 0.01	84.21 ± 0.0013	0.066 ± 0.004
In	0.95 ± 0.0005	^{115m}In	4.48 ± 0.004	336.2 ± 0.025	0.459 ± 0.001

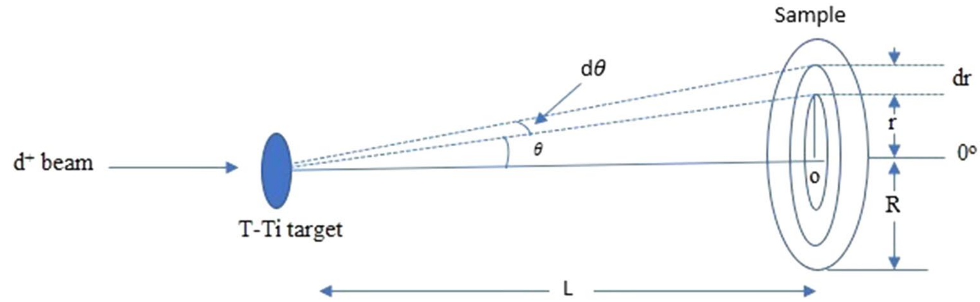

Fig. 2 Schematic representation of the experimental set up for the neutron induced reaction performed at the Purnima Neutron Generator (PNG) facility

titanium target loaded with tritium is employed as the neutron producing target. The operating parameters of the neutron generator for the experiment are 200 μA ion beam current and vacuum inside the system is maintained at pressure of 3E−6 mbar. One thorium metal foil of 0.72 cm^2 size and one indium monitor foil of 0.5 cm^2 size were taken for irradiation. The thicknesses of the thorium and indium foils are 0.017 mg/cm^2 and 0.068 mg/cm^2. The Th-metal foil and the In-monitor foils are 150.1 and 250.5 mg, respectively. The individual foils were wrapped with 0.025 mm thick super pure Al-foil and a stack was made. Then a stack of Al-wrapped Th and In metal foils were irradiated together for 5850 s using the neutron beam from the D+T reaction. The cooling time for irradiated Th and In foils are 73,937.0 s and 63,872 s, respectively. The γ-ray spectrometric analyses consisting of calibration of the HPGe detector followed by γ-ray counting of irradiated foils as mentioned in the above section. The counting time of the sample and monitor foils are 6624 and 7200 s, respectively.

Calculation of neutron energy

Effective neutron energy in the $^{7}Li(p,n)$ neutron source

The method of the calculation of effective neutron energies in a ^{7}Li(p, n) reaction are available in Refs. [9–11]. The proton energy degradation in the tantalum and lithium foils was calculated using SRIM software [12]. The degradation of energies for the proton beam of 13, 17 and 21 MeV in the front tantalum foil were about 0.061, 0.050 and 0.043 MeV, respectively. Similarly, the degradation of energies due to passage of protons in the lithium foil were about 0.11, 0.096 and 0.077 MeV, respectively. The information about the proton energy degradation in front tantalum and lithium foil is used in finding the average proton energy, E_p, which are 12.91 ± 0.04, 16.92 ± 0.03 and 20.93 ± 0.03 MeV, respectively.

Using the relation, $E_n^k = E_p - E_{th}$, the neutron energies E_n^k due to kinematics were obtained as 11.03 ± 0.04, 15.04 ± 0.03 and 19.05 ± 0.03 MeV, where E_{th} is the threshold energy of ^{7}Li(p, n) reaction (E_{th} = 1.881 MeV). Uncertainty in the neutron energy due to kinematics was obtained using the law of error propagation.

We obtain the neutron energies, E_n^{sp} from the neutron spectra corresponding to E_p of 13, 17 and 21 MeV, which are given in Ref. [13]. Mean values of E_n^{sp} corresponding to primary group of neutrons are obtained as weighted average of neutron energy with fluxes taken as weight and uncertainty assigned to E_n^{sp}. The uncertainty to E_n^{sp} was obtained based on FWHM taken from the spectrum corresponding to primary group of neutrons and then using relation "standard deviation = FWHM/2.3548". The neutron energies E_n^{sp} due to neutron spectra are obtained as 9.96 ± 0.58, 13.88 ± 0.51 and 17.67 ± 0.48 MeV, respectively.

The effective neutron energies are obtained by taking the average of the neutron energies, which were obtained by using kinematics (E_n^k) and spectra (E_n^{sp}). The effective neutron energies values are 10.49 ± 0.29, 14.46 ± 0.26 and 18.36 ± 0.24 MeV, respectively.

Neutron energy in the $^{3}H(d,n)$ neutron source

The method for the calculation of neutron energies in a ^{3}H(d, n) reaction is available in Ref. [14]. The datasets used in the calculation of this neutron energy is available in detail in Ref. [15] and the same is not reproduced here in order to save space. The neutron energy with its associated error is obtained as 15.03 ± 0.003 MeV.

Efficiency calibration of HPGe detector using the ^{133}Ba and ^{152}Eu standard γ-ray sources

The efficiency of the HPGe detector used in the experiments involving ^{7}Li(p, n) and ^{3}H(d, n) reaction as neutron sources is described below.

Efficiency calibration of detector in the experiment of $^{7}Li(p, n)$ neutron source

The calibration procedure for the HPGe detector used in the present work is carried out using a ^{133}Ba (Source activity = 64,860.96 ± 254.67 Bq as on 1-10-1999) and a ^{152}Eu (Source activity = 38,832.18 ± 197.05 Bq as on 1-10-1999) standard point sources. The standard point sources were situated at a suitable distance of 1 cm from the detector end cap. For the estimation of efficiency of HPGe detector system, following relation was used.

$$\varepsilon\left(E_{\gamma}\right) = \frac{CK_{C}}{I_{\gamma}A_{0}e^{-0.693t/T_{1/2}}} \quad (1)$$

where E_{γ} is γ-ray energy, $\varepsilon\left(E_{\gamma}\right)$ is efficiency, C is detected γ-ray counts per second, $T_{1/2}$ is half-life, t is elapsed time between date of manufacture of calibration source and detector calibration. The γ-ray abundance $\left(I_{\gamma}\right)$, half-life at each of the seven γ-ray energies of ^{133}Ba and ^{152}Eu, which were retrieved from Ref. [16]. The correction factor as a result of coincidence summing effect K_{C} was determined by using EFFTRAN code [17]. Table 2 presents the auxiliary data, experimental data of counts and the values for efficiencies ε_{i} of the detector for the 7 γ-lines.

The covariance matrix V_{ε} for the seven γ-ray energies versus efficiencies, were obtained using the micro correlation method of Smith [18], which was later followed by others [9, 10, 19]. The covariance matrix V_{ε} was obtained by considering the uncertainty information in each of the four attributes C, I_{γ}, A_{o} and $T_{1/2}$ and correlations between them. Partial uncertainties in ε_{i} due to attributes C, I_{γ}, A_{o} and $T_{1/2}$ are calculated and the result of the covariance analysis for efficiencies at these 7 energies, V_{ε} of order 7 × 7 corresponding to the ^{133}Ba and ^{152}Eu standard sources was obtained.

The characteristic γ-ray energies of the reaction product ^{231}Th and fission product ^{97}Zr are different from γ-ray energies of ^{133}Ba and ^{152}Eu sources. To determine the efficiencies of detector corresponding to the γ-rays of ^{231}Th and fission products ^{97}Zr, we considered following linear parametric function

$$Z = \text{In}\left(\varepsilon_{i}\right) = \sum_{k=1}^{m} p_{k}(\ln\left[E_{i}\right])^{k-1} \quad 1 \le i \le 10, \quad 1 \le k \le m \quad (2)$$

The goodness of fit was achieved for $n = 4$, with $\frac{\chi^{2}}{10-4} = 1.25 \approx 1$. We consider the following linear parametric model as the best model, which is given below.

$$\ln\varepsilon = -3.73 - 0.94\ln E + 0.09(\ln E)^{2} + 0.08(\ln E)^{3} \quad (3)$$

Equation (3) was used to estimate the efficiencies corresponding to γ-rays emitted from the reaction product ^{231}Th and fission product ^{97}Zr. The best values and covariance matrix for efficiency at characteristic γ-ray energy of 84.21 and 743.3 keV, can be accomplished by following the method of least squares. Table 3 contains information about the efficiency of HPGe detector ε_{γ_i} for 84.21 and 743.3 keV γ-lines of the reaction products ^{231}Th and ^{97}Zr corresponding to the sample and the monitor along with correlation matrix.

Efficiency calibration of detector in the experiment of $^{3}H(d, n)$ neutron source

The calibration procedure for the HPGe detector used in the present work is carried out using a ^{133}Ba (Source activity = 111,000 Bq as on 1-3-2006) standard point source

Table 2 Specification of γ-ray energy, γ-ray photo-peak counts, γ-ray abundance, half-life and efficiency of the detector for the experiment involving ^{7}Li(p, n) neutron source

γ-Ray energy (keV)	γ-Ray abundance (%)	Counts (s)	Half-life (y)	Efficiency ε_i
^{133}Ba				
80.9	32.9 ± 0.3	1333.96 ± 1.42	10.551 ± 0.011	0.1898 ± 0.0019
160.6	0.638 ± 0.005	45.50 ± 1.10		0.3339 ± 0.0086
^{152}Eu				
367.8	0.859 ± 0.006	13.03 ± 0.30	13.517 ± 0.014	0.0930 ± 0.0023
586.3	0.455 ± 0.004	4.0555 ± 0.33		0.0546 ± 0.0045
778.9	12.93 ± 0.08	66.365 ± 0.54		0.0315 ± 0.0004
964.1	14.51 ± 0.07	53.59 ± 0.4605		0.0226 ± 0.0003
1112.1	13.67 ± 0.08	38.44 ± 0.3266		0.0172 ± 0.0002

Table 3 Specification of interpolated detector efficiencies for the experiemnt involving ^{7}Li(p, n) neutron source

Radio-nuclide	γ-Ray energy (keV)	Efficiency (ε_{γ_i}); i = U, M	Correlation matrix	
^{231}Th	84.21 ± 0.0013	0.2151 ± 0.0024	1	
^{97}Zr	743.3 ± 0.03	0.0337 ± 0.0004	−0.04204	1

situated at the detector end cap. The time taken between the calibration, at the time of packing and at the time of the experiment was 11.7 years. Table 4 presents the auxiliary data, experimental data of counts and the values for efficiencies ε_i of the detector at 8 γ-lines. Partial uncertainties in ε_i due to attributes C, I_γ, A_o and $T_{1/2}$ are calculated and the result of the covariance analysis for efficiencies at these 8 energies, V_ε of order 8×8 corresponding to ^{133}Ba standard source. In this experiment also, the best values and covariance matrix for efficiency at characteristic γ-ray energies of 84.21 and 336.2 keV, can be accomplished by the method of least squares as mentioned before. Detailed description of the data sets used in the calculation of efficiency is given in Ref. [15]. Table 5 contains information about the efficiency of the HPGe detector ε_{γ_i} at 84.21 and 336.2 keV γ-lines of the reaction products ^{231}Th and ^{115m}In corresponding to the sample and the monitor.

Measurement and covariance analysis of the ^{232}Th$(n, 2n)^{231}$Th reaction cross section

The neutron induced reaction cross section at a particular neutron energy can be obtained using the relation,

$$\sigma_U = \sigma_M Y \frac{C_U \lambda_U Wt_M abn_M Av_U (I_\gamma)_M \varepsilon_{\gamma_M} \left(1 - e^{-\lambda_M t_{irrM}}\right)\left(e^{-\lambda_M t_{coolM}}\right)\left(1 - e^{-\lambda_M t_{cM}}\right)}{C_M \lambda_M Wt_U abn_U Av_M (I_\gamma)_U \varepsilon_{\gamma_U} \left(1 - e^{-\lambda_U t_{irrU}}\right)\left(e^{-\lambda_U t_{coolU}}\right)\left(1 - e^{-\lambda_U t_{cU}}\right)} \prod_k \frac{(C_k)_M}{(C_k)_U} \quad (4)$$

where U and M represent sample and monitor, $\sigma_U(E_n)$ and $\sigma_M(E_n)$ denote cross section at the neutron energy E_n; Y denotes yield of fission product in the neutron induced fission and is only taken into consideration for nuclides undergoing fission, C_U and C_M denote the detected γ-ray peak counts for the nuclides of target and monitor; λ_U, λ_M denote decay constants of the reaction product from the target and monitor; ε_{γ_U} and ε_{γ_M} denote the efficiencies of the detector corresponding to characteristic γ-rays of the product nuclides; Wt_U, Wt_M denote weights of the target and monitor; abn_U and abn_M denote isotopic abundances of target and monitor; Av_U, Av_M denote average atomic mass of target and monitor; $(I_\gamma)_U$ and $(I_\gamma)_M$ denote γ-ray abundances of the nuclides. t_{irr}, t_{cool} and t_c denote the irradiation time, cooling time and counting time of the target. $(C_k)_U$ and $(C_k)_M$ denote the correction factors for the kth attribute, where k represents the (a) dead time correction factor of the detector $\left[\left(\frac{CL}{LT}\right)_U, \left(\frac{CL}{LT}\right)_M\right]$, CL refers to clock time and LT refers to Live time, (b) low energy neutron contribution factor (α_U, α_M) and (c) γ-ray self-attenuation factor $[(\Gamma_{attn})_U, (\Gamma_{attn})_M]$ (d) Area (A_U, A_M) factor. The correction term in (a) can be obtained during the experiment through MCA. The correction term in (b) was obtained following the approach given originally by Smith et al. [20]. The correction term in (c) was obtained by using the expression, $\Gamma_{attn} = \frac{1-e^{-\mu l}}{\mu l}$, where l is the thickness of the sample and μ is mass attenuation coefficient obtained from XMuDat Ver. 101 [21, 22]. The covariance matrix for cross section at the required neutron energy was obtained using the relation,

$$V_{\sigma(U)} = \sum_{kl=1}^{n} P_k S_{kl} P_l; \quad 1 \le k, \quad l \le 18 \quad (5)$$

Table 4 Specification of γ-ray energy, γ-ray photo-peak counts, γ-ray abundance, half-life and efficiency of the detector for ^{133}Ba standard source for the experiment involving ^{3}H(d, n) neutron source

γ-Ray energy (keV)	γ-Ray abundance (%)	Peak area	Coincidence summing	Half-life (years)	Efficiency ε_i
53.1	2.14 ± 0.03	615 ± 150	1.348	10.551 ± 0.011	0.0038 ± 0.0009
80.9	32.9 ± 0.3	103,829 ± 322	1.286		0.0394 ± 0.0004
160.6	0.638 ± 0.005	3710 ± 222	1.049		0.0592 ± 0.0036
223.2	0.453 ± 0.003	1864 ± 129	1.203		0.0481 ± 0.0033
276.4	7.16 ± 0.05	27,920 ± 753	1.194		0.0452 ± 0.0013
302.8	18.34 ± 0.13	69,868 ± 2117	1.112		0.0412 ± 0.0013
356.0	62.05 ± 0.08	210,131 ± 7637	1.096		0.0361 ± 0.0013
383.8	8.94 ± 0.06	32,065 ± 886	0.891		0.0310 ± 0.0009

Table 5 Specification of interpolated detector efficiencies for the experiment involving ^{3}H(d, n) neutron source

Radio-nuclide	γ-Ray energy (keV)	Efficiency (ε_{γ_i}); i = U, M	Correlation matrix	
^{231}Th	84.21 ± 0.0013	0.0434 ± 0.0006	1	
^{115m}In	336.2 ± 0.025	0.0378 ± 0.0007	−0.04698	1

where $V_{\sigma(U)}$ denotes the covariance matrix for cross section, P_k and P_l denote the diagonal matrix for partial errors for n observations due to kth attribute and n observations due to lth attribute. S_{kl} denotes the micro-correlation matrix.

The ^{232}Th(n, 2n)^{231}Th reaction cross section in the experiment of ^{7}Li(p, n) neutron source

The ^{232}Th(n, 2n)^{231}Th reaction cross section for the neutron energies of 10.49, 14.46 and 18.36 MeV at the BARC-TIFR Pelletron facility were obtained by using Eq. (1). Numerical values for the attributes of cross section is mentioned in the detailed research gate internal log book document [15]. Among the attributes mentioned in Eq. (4), the attributes measured with error are $\sigma_M(E_n)$, C_U, C_M, λ_U, λ_M, Av_U, Av_M, Wt_U, Wt_M, $(I_\gamma)_U$, $(I_\gamma)_M$, ε_{γ_U}, ε_{γ_M}, $(\Gamma_{attn})_U$, $(\Gamma_{attn})_M$, A_U, A_M, Y. Other attributes namely, t_{irr}, t_{cool} and t_c given in Eq. (4) are observed without error and treated as constants. The data for cumulative yield Y of ^{97}Zr fission product in ^{232}Th(n, f) reaction with uncertainty (3.358 ± 0.134) was taken from Ref. [23]. The partial uncertainties for the three observations in all the 18 attributes of cross section are presented in Table 6. The monitor cross sections for the neutron induced fission of ^{232}Th was obtained from ENDF/B-V111.0 and then interpolated to obtain the cross section at the neutron energies of 10.49, 14.46 and 18.36 MeV. The data with necessary covariance information is presented in Table 7. The observations between any pair of attributes appearing in Eq. (1) are independent of each other except for the pairs of attributes (ε_{γ_U}, ε_{γ_M}), (Av_U, Av_M), (Wt_U, Wt_M), (A_U, A_M), ($(\Gamma_{attn})_U$, Wt_U), ($(\Gamma_{attn})_M$, Wt_M), ($(\Gamma_{attn})_U$, A_U) and ($(\Gamma_{attn})_M$, A_M) where $cor(\varepsilon_{\gamma_U}, \varepsilon_{\gamma_M}) = -0.4204$, $cor(Av_U, Av_M) = 1$, $cor(Wt_U, Wt_M) = 1$ and $cor(A_U, A_M) = 1$. There exists correlation between

Table 7 ^{232}Th(n, f)^{97}Zr and ^{115}In(n, n^{l})^{115m}In reaction cross sections with correlation matrix at their respective neutron energies

Neutron energy (MeV) (Experiment involving ^{7}Li(p, n) reaction as neutron source)	^{232}Th(n, f) reaction cross section (barn)	Correlation matrix
10.49 ± 0.29	0.310 ± 0.007	$\begin{bmatrix} 1 & & \\ 0.8939 & 1 & \\ 0.8943 & 0.8350 & 1 \end{bmatrix}$
14.46 ± 0.26	0.370 ± 0.009	
18.36 ± 0.24	0.480 ± 0.011	
Neutron energy (MeV) (Experiment involving ^{3}H(d, n) reaction as neutron source)	^{115}In(n, n^{l})^{115m}In reaction cross section (barn)	Correlation matrix
15.03 ± 0.003	0.058 ± 0.002	[1]

Table 6 Partial uncertainties in the ^{232}Th(n, 2n)^{231}Th reaction cross section

Attributes	Partial uncertainties in the ^{232}Th(n, 2n)^{231}Th reaction cross section (barn)			
	Experiment involving ^{7}Li(p, n) neutron source			Experiment involving ^{3}H(d, n) neutron source
	E_n = 10.49 MeV	E_n = 14.46 MeV	E_n = 18.36 MeV	E_n = 15.03 MeV
γ-Ray peak counts C_U	3.29E−02	1.58E−02	5.96E−03	6.49E−02
Decay constant λ_U	7.83E−04	5.53E−05	−1.53E−05	−1.61E−04
Average atomic mass Av_U	1.42E−08	7.14E−09	2.98E−09	6.83E−09
Isotopic abundance abn_M	NIL	NIL	NIL	5.43E−04
Weight of the sample Wt_U	2.95E−03	1.45E−03	5.30E−04	4.00E−04
γ-Ray abundance $(I\gamma)_U$	1.31E−01	6.58E−02	2.75E−02	6.30E−02
Efficiency of detector ε_{γ_U}	2.37E−02	1.19E−02	4.97E−03	1.39E−02
Monitor cross section σ_M	4.73E−02	2.46E−02	1.02E−02	3.86E−02
Yield Y	8.65E−02	4.34E−02	1.81E−02	NIL
γ-ray attenuation coefficient $(\Gamma_{attn})_M$	1.66E−03	6.86E−04	3.25E−04	1.82E−03
Area A_M	5.89E−02	2.95E−02	1.23E−02	2.83E−02
γ-Ray peak counts C_M	2.25E−01	7.19E−02	2.69E−02	7.00E−02
Decay constant λ_M	7.85E−04	3.81E−04	1.81E−04	3.93E−04
Average atomic mass Av_M	1.42E−08	7.14E−09	2.98E−09	1.09E−10
Weight of monitor Wt_M	2.95E−03	1.45E−03	5.30E−04	2.40E−04
γ-Ray abundance $(I_\gamma)_M$	3.72E−03	1.87E−03	7.79E−04	2.26E−03
Efficiency of detector ε_{γ_M}	2.32E−02	1.17E−02	4.87E−03	1.93E−02
γ-Ray attenuation coefficient $(\Gamma_{attn})_U$	3.27E−02	1.42E−02	6.52E−03	5.22E−02
Area A_U	5.89E−02	2.96E−02	1.23E−02	2.83E−02

$((\Gamma_{attn})_U, A_U)$, $((\Gamma_{attn})_M, A_M)$, $((\Gamma_{attn})_U, Wt_U)$, $((\Gamma_{attn})_M, Wt_M)$ corresponding to the 3 observations and the data are given in Ref. [15]. The observations of attributes C_U, C_M, Wt_U ,Wt_M, $(\Gamma_{attn})_U$, $(\Gamma_{attn})_M$, A_U and A_M with reference to different neutron energies are independent, therefore the corresponding micro-correlation matrices are identity matrices of size three. For the three observations in λ_U, λ_M, Av_M, Av_U, $(I_\gamma)_U$, $(I_\gamma)_M$, ε_{γ_U}, ε_{γ_M} and Y, the micro-correlation matrix corresponding to each of these attributes is equal to J matrix of order 3 with all entries equal to one. The data of σ_U with necessary covariance information is given Table 8. Hence the cross sections for the ^{232}Th(n, 2n)^{231}Th reaction with covariance error matrix was obtained by substituting the numerical values for the attributes and it's corresponding partial uncertainties.

The ^{232}Th(n, 2n)^{231}Th reaction cross section in the experiment of ^{3}H(d, n) neutron source

The ^{232}Th(n, 2n)^{231}Th reaction cross section for the neutron energy of 15.03 MeV at the Purnima neutron generator facility were obtained using Eq. (4). Numerical values for the attributes of cross section is mentioned in the detailed research gate internal log book document [15]. Among the attributes mentioned in Eq. (1), the attributes measured with error are $\sigma_M(E_n)$, C_U, C_M, λ_U, λ_M, Av_U, Av_M, Wt_U, Wt_M, $(I_\gamma)_U$, $(I_\gamma)_M$, ε_{γ_U}, ε_{γ_M}, $(\Gamma_{attn})_U$, $(\Gamma_{attn})_M$, A_U, A_M, abn_M. Other attributes namely, t_{irr}, t_{cool} and t_c given in Eq. (4) are observed without error and treated as constants. The partial uncertainties for the 1 observation in all the 18 attributes of cross section are presented in Table 6. The cross sections for the ^{115}In(n, n^{l})^{115m}In monitor reaction was obtained from IRDFF v.1.05 [24] and then interpolated to obtain cross section at neutron energy of 15.03 MeV. The data with necessary covariance information is presented in Table 7. The observation between any pair of attributes appearing in Eq. (1), $(\varepsilon_{\gamma_U}, \varepsilon_{\gamma_M})$, (Av_U, Av_M), (Wt_U, Wt_M), (A_U, A_M), $((\Gamma_{attn})_U, Wt_U)$, $((\Gamma_{attn})_M, Wt_M)$, $((\Gamma_{attn})_U, A_U)$ and $((\Gamma_{attn})_M, A_M)$ are dependent where $cor(\varepsilon_{\gamma_U}, \varepsilon_{\gamma_M}) = -0.04698$, $cor(Av_U, Av_M) = 1$, $cor(Wt_U, Wt_M) = 1$ and $cor(A_U, A_M,) = 1$. There exists correlation between $((\Gamma_{attn})_U, A_U)$, $((\Gamma_{attn})_M, A_M)$, $((\Gamma_{attn})_U, Wt_U)$, $((\Gamma_{attn})_M, Wt_M)$ corresponding to the 3 observations and the data are given in Ref. [15]. For each of the attributes, C_U, C_M, λ_U, λ_M, Av_U, Av_M, $(I_\gamma)_U$, $(I_\gamma)_M$, ε_{γ_U}, ε_{γ_M}, Wt_U, Wt_M, $\sigma_M(E_n)$, abn_M, $(\Gamma_{attn})_U$, $(\Gamma_{attn})_M$, A_U and A_M the micro-correlation within itself is equal to one. The data of σ_U with necessary covariance information is given Table 8. Hence the cross sections for ^{232}Th(n, 2n)^{231}Th reaction with covariance error matrix was obtained by substituting the numerical values for the attributes and its corresponding partial uncertainties.

Table 8 Experimentally measured ^{232}Th(n, 2n)^{231}Th reaction cross sections with correlation matrix

Neutron energy (MeV) (Experiment involving ^{7}Li(p, n) neutron source)	^{232}Th(n, 2n)^{231}Th reaction cross section (barn)	Correlation matrix
10.49 ± 0.29	2.16 ± 0.31	$\begin{bmatrix} 1 & & \\ 0.34 & 1 & \\ 0.31 & 0.37 & 1 \end{bmatrix}$
14.46 ± 0.26	1.08 ± 0.13	
18.36 ± 0.24	0.45 ± 0.06	
Neutron energy (MeV) (Experiment involving ^{3}H(d, n) neutron source)	^{232}Th(n, 2n)^{231}Th reaction cross section (barn)	Correlation matrix
15.03 ± 0.003	1.04 ± 0.14	[1]

Discussion

In the present study, the cross sections of ^{232}Th(n, 2n)^{231}Th reaction relative to the ^{232}Th(n, f)^{97}Zr monitor reaction at the effective neutron energies of 10.49 ± 0.29, 14.46 ± 0.26, 18.36 ± 0.24 MeV and relative to the ^{115}In(n, n^{l})^{115m}In monitor reaction at the neutron energy of 15.03 ± 0.003 MeV were measured by using the activation method and off-line γ-ray spectrometric technique. The uncertainty in the reaction cross sections was performed by using the method of covariance analysis. The ^{232}Th(n, 2n)^{231}Th reaction cross-section at the average neutron energy of 18.36 ± 0.24 MeV was determined for the first time.

For comparison, we present our data in Fig. 3 along with the data from EXFOR [25] compilation, where literature data [26–47] are available. In the same figure, we have also plotted the evaluated data curves from the ENDF/B-VIII.0 [48], JENDL 4.0 [49], JEFF-3.2 [50], ROSFOND-2010 [51], TENDL-2017 [52] libraries and the theoretical values based on TALYS-1.9 [53]. It can be seen from Fig. 3 that the ^{232}Th(n, 2n)^{231}Th reaction cross-section within the neutron energies of 10–12 MeV are very much scattered and there is significant differences between the some of the literature data and present data. The value from the present work at the neutron energy of 10.49 ± 0.29 MeV is on the lower side but in close agreement with the results of Tewes et al. [40]. Our measured cross section value for the ^{232}Th(n, 2n)^{231}Th reaction at the neutron energy of 10.49 ± 0.29 MeV agrees well with the evaluated data from ENDF/B-VIII.0, JENDL 4.0, JEFF-3.2, ROSFOND-2010 and theoretical value from TALYS-1.9. The ^{232}Th(n, 2n)^{231}Th reaction cross sections at the neutron energy of 14.46 ± 0.26 MeV in the experiment involving ^{7}Li(p, n) reaction neutron source is in agreement with the evaluated data of JEFF-3.2, ROSFOND-2010, TENDL-2017 and the literature data. Similarly, the present result at the neutron energy of 15.03 ± 0.003 MeV in the experiment involving ^{3}H(d, n) reaction neutron source is

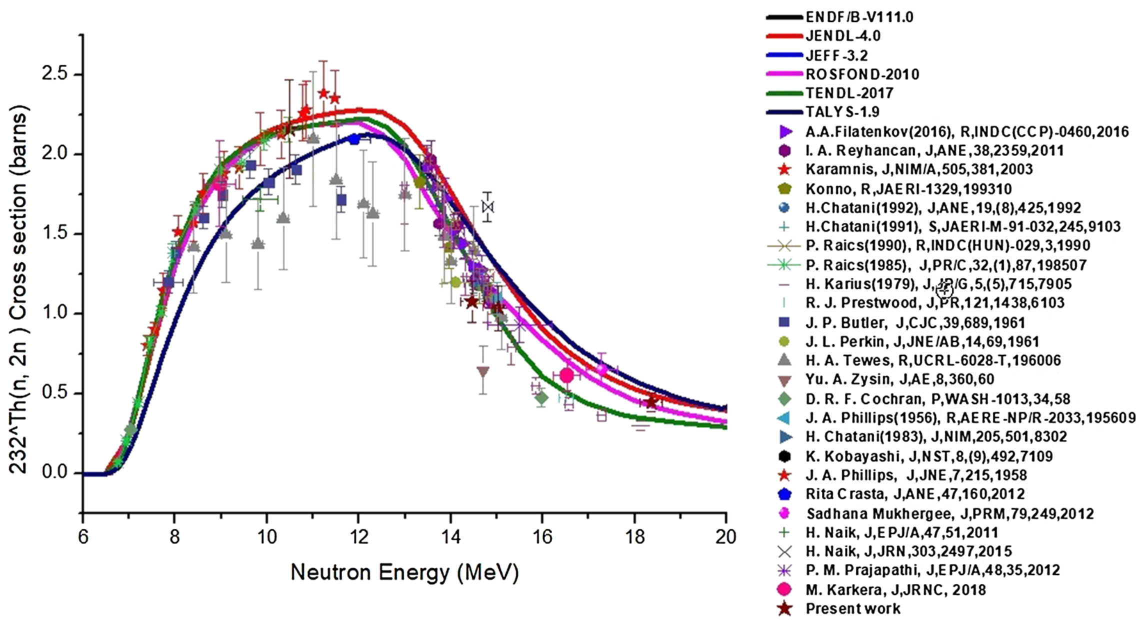

Fig. 3 Representation of the ^{232}Th(n, 2n)^{231}Th reaction cross section as a function of neutron energy

also in agreement with the evaluated data of JEFF-3.2, ROSFOND-2010, TENDL-2017 and the literature data. On the other hand, the ^{232}Th(n, 2n)^{231}Th reaction cross section at the neutron energy of 18.36 ± 0.24 MeV based on the ^{7}Li(p, n) reaction neutron source is in good agreement with the evaluated data of ENDF/B-VIII.0, JENDL 4.0 and ROSFOND-2010.

The ^{232}Th(n, 2n)^{231}Th reaction cross sections with accurate uncertainties at different neutron energies of present work and literature data will be helpful for an evaluator to generate a recommended data file. The ^{232}Th(n, 2n)^{231}Th reaction cross sections at different neutron energies are useful for the design of various types of reactors such as advanced heavy water reactor (AHWR) [3] and accelerated driven subcritical system (ADSs) [4–6].

Conclusion

The cross sections of ^{232}Th(n, 2n)^{231}Th reaction at the effective neutron energies of 10.49 ± 0.29, 14.46 ± 0.26, 18.36 ± 0.24 MeV and 15.03 ± 0.003 MeV were measured by using the activation method and off-line γ-ray spectrometric technique. The result from the present work at the neutron energy of 18.36 ± 0.24 MeV is determined for the first time, whereas for others are in agreement with most of the literature data. The present data at the neutron energies of 10.49 ± 0.29 MeV, 14.46 ± 0.26 MeV, 15.03 ± 0.01 MeV and 18.36 ± 0.24 MeV are also in agreement with most of the evaluated data of ENDF/B-VIII.0, JENDL 4.0, JEFF-3.2, ROSFOND-2010 and TENDL-2017 nuclear data libraries as well as with the calculated data based on TALYS-1.9 code. The ^{232}Th(n, 2n)^{231}Th reaction cross sections with appropriate uncertainties at different neutron energies are important for the design of different advanced reactors.

Acknowledgements The research work was supported by DAE-BRNS project (Sanction No. 36(6)/14/52/2014-BRNS/2708). The authors would like to thank the staff of BARC-TIFR Pelletron facility and PURNIMA neutron generator facility for their kind co-operation in providing the proton beam to carry out the experiment. One of the authors, Meghna Karkera gratefully acknowledges the Department of Atomic Energy of India for the award of Senior Research Fellowship to carry out the study. Meghna Karkera would also like to thank Dr. Mahesha, MIT, Manipal and colleague Savita for their timely guidance.

References

1. Allen TR, Crawford DC (2007) Sci Tech Nucl Install, Article ID 97486
2. Reactors Accelerator Driven Systems Knowledge Base (2002) Thorium fuel utilization: options and trends. IAEA-TECDOC-1319
3. Sinha RK, Kakodkar A (2006) Nucl Eng Des 236:683–700
4. Carmati F, Klapisch R, Revol JP, Roche C, Rubio JA, Rubia C (1993) CERN/AT/93-47
5. Rubbia C, Roche C, Rubio JA, Carminati F, Kadi Y, Mandrillon P, Revol JP, Buono S, Klapisch R, Fiétier N, Gelès C (1995) CERN-AT-95-44-ET
6. Bowman CD (1998) Annu Rev Nucl Part Sci 48:505–556
7. BARC-TIFR Pelletron LINAC Facility. http://www.tifr.res.in/pell/pelletron/index.php
8. PURNIMA Neutron Generator. The plutonium reactor for neutronic investigations in multiplying assemblies. https://www.nti.org/learn/facilities/861/

9. Shivashankar BS, Ganesan S, Naik H, Suryanarayana SV, Nair NS, Prasad KM (2015) Nucl Sci Eng 4:423–433
10. Yerraguntla SS, Naik H, Karantha MP, Ganesan S, Suryanarayana SV, Badwar S (2017) J Radioanal Nucl Chem 314:457–465
11. Meghna K, Naik H, Punchithaya S, Prasad KM, Yeraguntla SS, Suryanarayana SV, Ganesan S, Vansola V, Makhwana R (2018) J Radioanal Nucl Chem 318:1893–1900
12. Ziegler JF (2016) SRIM-2013. Pergamon, New York, p 2013
13. Poppe CH, Anderson JD, Davis JC, Grimes SM, Wong C (1976) Phys Rev C 14:438
14. Luo J, Du L, Zhao J (2013) Beam interactions with materials and atoms. Nucl Instrum Methods Phys Res B 298:61–65
15. Meghna K, Naik H, Yeraguntla SS, Punchithaya S, Dhanu LS, Prasad KM, Rajeev K, Kapil D, Devesh R, Tarun P, Saroj B, Suryanarayana SV, Ganesan S, Umasankari K (2019) Tech report no 5. https://www.researchgate.net/publication/332876423_Detailed_covariance_analysis_in_the_measurement_of_cross_sections_for_the_232Thn_2n231Th_reaction_at_the_effective_neutron_energies_of_1049029_MeV_1446026_MeV_1836024_MeV_and_15030003_MeV_using_the_7Li
16. NuDat 2.7 (2016) National Nuclear Data Center, Brookhaven National Laboratory. http://www.nndc.bnl.gov/nudat2
17. Vidmar T (2005) EFFTRAN—a Monto Carlo efficiency transfer code for gamma-ray spectrometry. Nucl Instrum Methods Phys Res A 550:603
18. Smith DL (1987) Accelerators, spectrometers, detectors and associated equipment. Nucl Instrum Methods Phys Res A 257:365–370
19. Karkera M, Naik H, Yeraguntla SS, Vansola V, Suryanarayana SV, Prasad KM, Ganesan S, Punchithaya S (2018) RG tech report no 4. https://www.researchgate.net/publication/329527685_Detailed_data_sets_related_to_the_covariance_analysis_of_the_measurement_of_cross_section_data_of_232Thn_2n231Th_reaction
20. Smith DL, Plompen AJ, Semkova V (2005) Organisation for Economic Co-operation and Development-Nuclear Energy Agency (NEA/WPEC-19, ISBN 92-64-01070-X)
21. Nowotny R (2018) IAEA Rep. IAEA-NDS 195. https://www-nds.iaea.org/publications/iaea-nds/iaea-nds-0195.htm
22. Millsap DW, Landsberger S (2015) Appl Radiat Isot 97:21–23
23. Sonzogni A (2008) National nuclear data centre. Brookhaven National Laboratory, pp 103–118. https://www.nndc.bnl.gov/
24. Zsolnay EM, Capote NR, Nolthenius HJ, Trkov A (2014) International reactor dosimetry and fusion file (IRDFF v1.05). https://www-nds.iaea.org/IRDFF/
25. Otuka N, Dupont E, Semkova V, Pritychenko B, Blokhin AI, Aikawa M, Babykina S, Bossant M, Chen G, Dunaeva S, Forrest RA (2014) Nucl Data Sheets 120:272–276
26. Filatenkov AA (2016) USSR report to INDC, CCP-0460
27. Reyhancan IA (2011) Ann Nucl Energy 38:2359–2362
28. Karamanis D, Andriamonje S, Assimakopoulos PA, Doukellis G, Karademos DA, Karydas A, Kokkorir M, Kossionides S, Nicolis NG, Papachristodoulou C, Papadopoulos CT (2003) Accelerators, spectrometers, detectors and associated equipment. Nucl Instrum Methods Phys Res A 505:381–384
29. Konno C, Ikeda Y, Oishi K, Kawade K, Yamamoto H, Maekawa H (1993) JAERI1329
30. Chatani H, Kimura I (1992) Ann Nucl Energy 19:425–429
31. Chatani H, Kimura I (1991) JAERI-M-91-032
32. Raics P, Nagy S, Daroczy S, Kornilov NV (1990) International Atomic Energy Agency
33. Raics P, Daroczy S, Csikai J, Kornilov NV, Baryba VY, Salnikov OA (1985) Phys Rev C 32:87
34. Chatani H (1983) Nucl Instrum Methods Phys Res 205:501–504
35. Karius H, Ackermann A, Scobel W (1979) J Phys G (Nucl Phys) 5:715
36. Kobayashi K, Hashimoto T, Kimura I (1971) J Nucl Sci Technol 8:492–497
37. Prestwood RJ, Bayhurst BP (1961) Phys Rev 121:1438
38. Perkin JL, Coleman RF (1961) J Nucl Energy Parts A/B React Sci Technol 14:69–75
39. Butler JP, Santry DC (1961) Can J Chem 39(3):689–696
40. Tewes HA, Caretto AA, Miller AE, Nethaway DR (1960) California Univ Livermore (USA), Lawrence Livermore Lab
41. Zysin YA, Kovrizhnykh AA, Lbov AA, Sel'chenkov LI (1961) At Energy 8:310
42. Phillips JA (1958) J Nucl Energy 7:215–219
43. Naik H, Prajapati PM, Surayanarayana SV, Jagadeesan KC, Thakare SV, Raj D, Mulik VK, Sivashankar BS, Nayak BK, Sharma SC, Mukherjee S (2011) Eur Phys J A 47:51
44. Prajapati PM, Naik H, Suryanarayana SV, Mukherjee S, Jagadeesan KC, Sharma SC, Thakre SV, Rasheed KK, Ganesan S, Goswami A (2012) Eur Phys J A 48:35
45. Crasta R, Naik H, Suryanarayana SV, Shivashankar BS, Mulik VK, Prajapati PM, Sanjeev G, Sharma SC, Bhagwat PV, Mohanty AK, Ganesan S, Goswami A (2012) Ann Nucl Energy 47:160–165
46. Mukerji S, Naik H, Suryanarayana SV, Chachara S, Shivashankar BS, Mulik V, Crasta R, Samanta S, Nayak BK, Saxena A, Sharma SC (2012) Pramana 79:249–262
47. Naik H, Surayanarayana SV, Bishnoi S, Patel T, Sinha A, Goswami A (2015) J Radioanal Nucl Chem 303:2497–2504
48. Chadwick MB, Herman M, Obložinský P, Dunn ME, Danon Y, Kahler AC, Smith DL, Pritychenko B, Arbanas G, Arcilla R, Brewer R (2011) ENDF/B-VIII. 0 nuclear data for science and technology: cross sections, covariances, fission product yields and decay data. Nucl Data Sheets 112:2887–2996
49. Shibata K, Iwamoto O, Nakagawa T, Iwamoto N, Ichihara A, Kunieda S, Chiba S, Furutaka K, Otuka N, Ohasawa T, Murata T, Matsunobu H, Zukeran A, Kamada S, Katakura J (2011) JENDL-4.0: a new library for nuclear science and engineering. J Nucl Sci Technol 48:1–30
50. Koning AJ, Bauge E, Dean CJ, Dupont E, Fischer U, Forrest RA, Jacqmin R, Leeb H, Kellett MA, Mills RW, Nordborg CM, Pescarini Rugama Y, Rullhusen P (2011) Status of the JEFF nuclear data library. J Korean Phys Soc 59(2):1057–1062
51. Zabrodskaya SV, Ignatyuk AV, Koscheev VN (2007) ROSFOND-Rossiyskaya Natsionalnaya Biblioteka Nejtronnykh Dannykh, In: VANT, Nuclear Constants 1–2
52. Rochman D, Koning AJ, Sublet JC, Fleming M, Bauge E, Hilaire S, Romain P, Morillon B, Duarte H, Goriely S, Van Der Marck SC (2017) The TENDL library: hope, reality and future. In: EPJ web of conferences. EDP Sciences, p 146
53. Koning AJ, Hilaire S, Goriely S (2015) TALYS-1.9, A nuclear reaction program. http://www.talys.eu/download-talys